Polish J. Chem., **74**, 1533–1566 (2000) **REVIEW ARTICLE**

Quantitative Surface Analysis by X-ray Photoelectron Spectroscopy

by A. Jabłoński

Institute of Physical Chemistry, Polish Academy of Sciences, ul. Kasprzaka 44/52, 01-224 Warsaw, Poland

(Received June 13th, 2000; revised manuscript August 2nd, 2000)

X-ray photoelectron spectroscopy (XPS) has become a powerful tool to study first few atomic layers at solid surfaces. This technique provides information on chemical state of atoms at the solid surface and the composition of the analysed layer. Present work reviews the typical procedures of quantitative XPS analysis. The relatively accurate procedures are based on measurements involving standards, *i.e.* samples with known surface composition. However, these procedures may be applicable to perfect samples with similar surface structure as the standards. In general, such approach is impractical for use in routine analysis of samples consisting of large number of components. In experimental practice we frequently encounter imperfect samples with rough surfaces, or in a form of a powder, for which the use of standards is not recommended. A convenient procedure to use in such a case is the relative sensitivity factor approach, which does not require the external standards. However, accuracy of this method is rather poor. A reasonable compromise for XPS analysis of complex samples is a variation of the relative sensitivity factor aproach with sensitivity factors determined for a given instrument and the used XPS configuration. A good example of the modification of the relative sensitivity factor approach is the multiline approach. The surface composition is calculated then after statistical analysis of all intensities observed in the spectra. The details of such procedure are discussed in the present review.

Key words: formalism of quantitative analysis, relative sensitivity factors, photoelectron transport in solids, inelastic mean free path, elastic photoelectron scattering, spectrometer function

1. INTRODUCTION

The X-ray photoelectron spectroscopy (XPS) seems to be the most universal method for quantitative analysis of solid surfaces, since this technique can be routinely applied to practicaly all types of samples, including poor conductors. This method has been elaborated in mid Sixties [1], and until now has become one of the most popular tools of surface science. Originally, this technique was designated with the acronim ESCA (Electron Spectroscopy for Chemical Analysis). Importance of ESCA-XPS has been recognized by awarding the Nobel Prize to its developer (K. Siegbahn in 1981).

Experiment associated with XPS consists in irradiating the surface studied with a beam of monochromatic X-rays and recording the energy distribution of electrons emitted from the surface. Two energies of X-rays are commonly used in experimental

practice: 1253.6 eV (Mg Kα) and 1486.6 eV (Al Kα). The kinetic energy of emitted electrons is obviously smaller than the exciting energy. Photoelectrons with such energies are created in the sample within the layer of the thickness of several μm. However, they can reach the surface without energy loss only when emitted within first few monolayers, due to a large cross section for inelastic scattering at these kinetic energies. In effect XPS becomes a surface sensitive technique, providing the qualitative and quantitative information for first atomic layers. The sampling depth of XPS is related to the inelastic mean free path of photoelectrons in the surface region, which typically varies from 4 Å to 20 Å depending on the photoelectron energy and on the solid studied. The qualitative and quantitative information on the composition of the analysed layer can be derived by proper processing of the energy spectra obtained. At present an extensive literature is available on the principles of XPS, analytical procedures and the necessary instrumentation. Material published up to 1990 is reviewed in the monograph edited by Briggs and Seah [2].

An example of the energy spectra recorded for the carefully cleaned surface of the Au50Pd50 alloy is shown in Fig. 1. The energy scale is usually expressed in terms of the so called binding energy, defined as the work necessary to transfer an electron in the solid to the Fermi level. For a given core level in the atom of a studied sample, the photoionization process is described by the energy conservation principle

$$E_{bf} = h\nu - E_{kv} - \varphi_{sa} \tag{1.1}$$

where E_{bf} is the binding energy, $h\nu$ is the energy of incident photons, E_{kv} is the photoelectron kinetic energy referenced to the vacuum level, and φ_{sa} is the work function for the sample material. However, the work function for the spectrometer material, φ_{sp}, may be different from φ_{sa}. Consequently, the kinetic energy of the emitted photoelectron, when entering the analyser, will be modified from E_{kv} to E'_{kv}

$$E'_{kv} = E_{kv} + (\varphi_{sp} - \varphi_{sa}) \tag{1.2}$$

i.e. will be accelerated or retarded by the contact potential $\Delta\varphi = \varphi_{sp} - \varphi_{sa}$. Introducing (1.2) into (1.1), we obtain

$$E_{bf} = h\nu - E'_{kv} - \varphi_{sp} \tag{1.3}$$

As one can see, the value of the binding energy does not depend on the sample work function. Thus, the Fermi level is a convenient reference for the energy scale. Calibration of the energy scale is an important procedure, especially for the qualitative applications of XPS. From positions of peaks one can identify the elements present in the

surface region. Furthermore, slight shifts of the peak positions provide further information on the chemical state of these elements. Detailed description of the calibration procedures can be found in [2, Appendix 1].

As indicated in Fig. 1, two most pronounced features of the spectrum can be ascribed to Pd 3d and Au 4f core level photoelectrons. Other features are due to Pd MNN Auger transition and to the valence band (v. b.). The latter features usually are not considered in the XPS quantitative analysis. Present work will be devoted to procedures of deriving the quantitative information from the core level peaks.

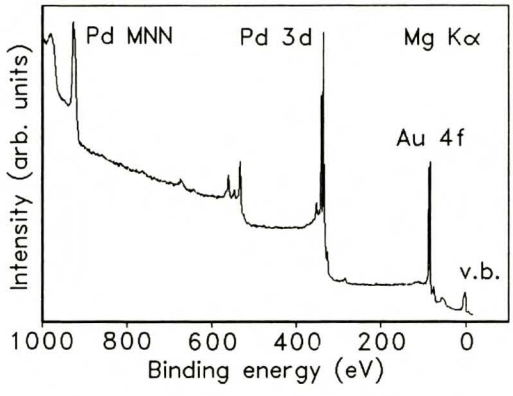

Figure 1. The energy spectra of electrons emitted from the Au50Pd50 alloy by the Mg Kα radiation.

Let us look more closely on the core level peaks shown in Fig. 1. The Au 4f photoelectron peak is shown in Fig. 2(a). One can see actually two peaks corresponding to the spin-orbit (*j-j*) coupling. Both peaks are characterized by the quantum number $j = l + s$. In the case considered, $l = 3$, and $s = \pm 1/2$, thus $j = 5/2$ and $7/2$. The procedure of quantitative analysis of a solid surface (*e.g.* the surface of the Au50Pd50 bulk alloy) derives the surface composition from the monitored peak intensities. First stage of the spectrum processing requires the removal of the contribution of secondary electrons. There are several algorithms commonly used for this purpose. In the simplest approach, illustrated in Fig. 2(b), the background is approximated by a straight line. After background subtraction the remaining spectrum is integrated within the selected limits. In the next stage the calculated area (or areas of several peaks) is used in calculations of the surface composition. These calculations require a theoretical model describing the photoelectron emission from a particular solid, taking into account a given experimental configuration.

Present work is devoted mainly to the overview of the procedures of quantitative analysis by XPS. Stress is put on analysis of complex multicomponent samples, which are frequently encountered in analytical practice. This problem is of considerable importance in routine applications of XPS. The structure of the paper is as follows: The commonly accepted formalism and the typical experimental procedures are described in Section 2. Quantitative analysis of complex multicomponent solids

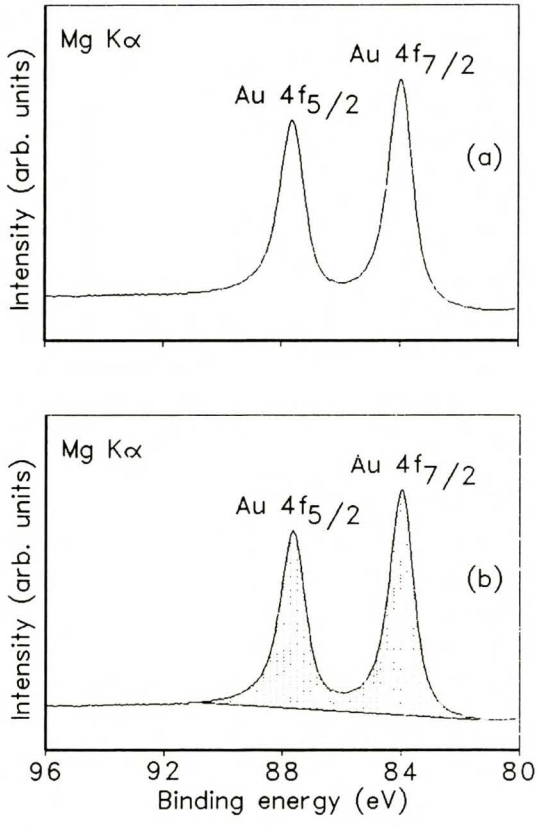

Figure 2. Fragment of the spectra shown in Fig. 1. (a) The Au 4f peak; (b) the same peak with indicated linear background and the integrated area.

and it reliability are discussed in Sections 3 and 4. A crucial step of quantitative XPS analysis is the signal intensity calibration by determining the so-called spectrometer function. This issue is addressed in Section 5. Improvements of the theory of electron transport by considering the elastic photoelectron scattering in the solid and energy dependence of the electron inelastic mean free path are summarized in Sections 6 and 7. Finally, a software packet with a convenient implementation of algorithms for quantitative XPS analysis is briefly described.

2. MATHEMATICAL FORMALISM OF XPS

In 1974, Fadley *et al.* [3] published an extensive theoretical background for quantitative XPS analysis. With minor modifications the mathematical formulation of photoelectron transport proposed by these authors is commonly used until present time. Let us list below the main assumptions of this formalism: 1. The solid surface is ideally flat. 2. The studied specimen is polycrystalline or amorphous. 3. The photoelectron attenuation within the solid is exponential. 4. The effect of elastic photoelec-

tron collisions in the solid on the angular distribution of emitted photoelectrons is negligible. 5. The sample in-depth composition is uniform. 6. The X-ray refraction and the reflection are neglected. 7. The X-ray attenuation within the analysed volume is negligible.

Under the above assumptions, the contribution to the recorded signal strength, dI, corresponding to the layer of thickness dz at the depth z is given by

$$dI = TD_e F_x A \Delta\Omega N (d\sigma_x/d\Omega) \exp[-z/(\lambda \cos\alpha)] dz \tag{2.1}$$

where T is the analyser transmission function, D_e is the detector efficiency, F_x is the flux of incident X-rays, A is the analysed area, $\Delta\Omega$ is the solid acceptance angle of the analyser, N is the atomic density of a given element (number of atoms in unit volume), α is the detection angle with respect to the surface normal, and λ is the inelastic mean free path of analysed photoelectrons (IMFP), *i.e.* the average distance between inelastic photoelectron collisions. The parameter $d\sigma_x/d\Omega$ denotes the differential photoelectric cross section. For unpolarized radiation and random orientation of atoms or molecules this cross section is expressed by [4,5]

$$d\sigma_x/d\Omega = \sigma_x W(\beta,\psi) = \sigma_x \frac{1}{4\pi}\left[1 - \frac{\beta}{4}\left(3\cos^2\psi - 1\right)\right] \tag{2.2}$$

where σ_x is the total photoelectric cross section, ψ is the angle between the direction of the X-rays and the direction of analysis, and β is the so-called asymmetry parameter. The function $W(\beta,\psi)$ is the photoelectric cross section normalized to unity, *i.e.*

$$2\pi \int_0^{\pi} W(\beta,\psi) \sin\psi \, d\psi = 1$$

The cross section $W(\beta,\psi)$ is shown in Fig. 3. As one can see, the cross section depends considerably on the asymmetry parameter, β. When $\beta = 0$, photoelectrons are emitted isotropically in space. However, with a few exceptions, the asymmetry parameter is larger than zero for photoelectrons emitted by the usually used radiations, *i.e.* Al Kα and Mg Kα [5–7]. In that case the maximum probability of photoemission is in the direction perpendicular to the direction of X-rays, as shown in Fig. 3. Maximum anisotropy is expected for the asymmetry parameter equal to 2. Such a value corresponds to photoelectrons emitted from the *s*-levels of low and medium atomic number elements.

In the typical experimental configuration of XPS, a semi-infinite solid is exposed to a broad beam of X-rays irradiating a much larger area than the area being analysed. We may then assume that the analysed area depends on the detection angle, α, according to

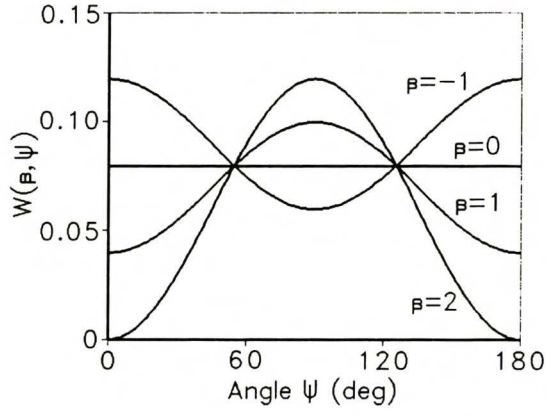

Figure 3. The normalized photoelectric cross section, $W(\beta,\psi) = (d\sigma_x/d\Omega)/\sigma_x$, as a function of the asymmetry parameter, β.

$$A = A_0/\cos\alpha \tag{2.3}$$

where A_o is the area seen by the analyser at the normal direction of analysis. On integration of (2.1) over all depths with account of (2.3), we obtain

$$I = TD_eA_0F_x\Delta\Omega N\lambda(d\sigma_x/d\Omega) \tag{2.4}$$

Equation (2.4) is the basis for calculations of the surface composition. As follows from assumption no 5, the above formalism applies to samples with uniform composition within the analysed volume. If this assumption is not strictly satisfied, all the procedures of quantitative XPS analysis described below would provide the averaged composition.

Exact algorithm for calculating the surface composition depends on the selected method of quantitative analysis. In general, there are two groups of experimental procedures used for this purpose: (i) analysis using standard materials, and (ii) the relative sensitivity factor approach. Let us briefly discuss both groups.

2.1. Quantitative analysis using standard materials

Presently, the most reliable quantitative applications of XPS, based on the above formalism, involve the use of standards, *i.e.* the use of samples with known surface composition. An obvious selection for a standard is the surface of a clean element, which is present in the sample studied. The simplest experimental procedure of quantitative analysis consists in measurements of a given peak intensity for a sample and for the standard. Let us write (2.4) for surface studied in the following way

$$I = CN\lambda = CM\lambda x \tag{2.5}$$

where x is the atom fraction of a given element, M is the total atomic density and the constant C comprises the parameters independent of composition

$$C = TD_e A_0 F_x \Delta\Omega(d\sigma_x/d\Omega)$$

Similarly, we have for the standard

$$I^0 = CM^0\lambda^0 \tag{2.6}$$

From (2.5) and (2.6) we obtain the following expression for calculating the surface composition of the element considered

$$\frac{I}{I^0} = \left(\frac{M}{M^0}\right)\left(\frac{\lambda}{\lambda^0}\right)x \tag{2.7}$$

Thus, the surface concentration of a given element can be calculated from the ratios of peak intensities, I/I^0, after correcting for differences in the inelastic mean free path and the atomic density for the sample and in the standard.

The described above simple procedure of quantitative analysis provides the surface concentration of one element. To obtain the total composition, we should use several standards corresponding to all elements present in the sample. (2.7) for the j-th element can be written as follows

$$x_j = \left(\frac{I_j}{I_j^0}\right)\left(\frac{M_j^0}{M}\right)\left(\frac{\lambda_j^0}{\lambda_j}\right) \tag{2.8}$$

The obvious condition has to be satisfied

$$\sum_{i=1}^{n} x_i = \sum_{i=1}^{n}\left(\frac{I_i}{I_i^0}\right)\left(\frac{M_i^0}{M}\right)\left(\frac{\lambda_i^0}{\lambda_i}\right) = 1 \tag{2.9}$$

From (2.8) and (2.9), on elimination of the atomic density of the sample, M, we obtain

$$x_j = \frac{1}{\sum_{i=1}^{n} \frac{(I_i/I_j)}{(I_i^0/I_j^0)F_{ij}}} = \frac{1}{\sum_{i=1}^{n} \frac{(I_i/I_i^0)}{(I_j/I_j^0)F_{ij}}} \tag{2.10}$$

where

$$F_{ij} = \left(\frac{\lambda_i}{\lambda_j}\right)\left(\frac{\lambda_j^0}{\lambda_i^0}\right)\left(\frac{M_j^0}{M_i^0}\right) \tag{2.11}$$

As follows from (2.10), two experimental procedures can be suggested. We can measure the ratios I_i/I_j for combinations of all elements present in the sample, and then the corresponding ratios for standards, I_i^0/I_j^0, in a separate experimental run. In the second procedure, we measure all the ratios I_i/I_i^0 for all elemental constituents of the sample.

For two component sample, *AB*, (2.10) and (2.11) simplify to

$$x_A = \frac{(I_A/I_A^0)}{(I_A/I_A^0) + (1/F_{AB})(I_B/I_B^0)} \tag{2.12}$$

where

$$F_{AB} = \left(\frac{\lambda_B}{\lambda_A}\right)\left(\frac{\lambda_A^0}{\lambda_B^0}\right)\left(\frac{M_A^0}{M_B^0}\right) \tag{2.13}$$

The procedures of quantitative XPS analysis can be based not only on elemental standards. In general, a standard sample may be a complex solid with a known surface composition reasonably close to the composition of the samples studied. Such a surface may be obtained by the vacuum fracture of a given compound or an alloy, or by scraping their surface. One can then assume that the composition of a newly created surface is close to the bulk composition. However, the applicability of such standards is limited to samples consisting of the same elements.

For simplicity, let us limit the formalism to the two component solids, *AB*. From (2.5) written for photoelectron emitted from both components of the sample, we obtain

$$\frac{I_A}{I_B} = \left(\frac{C_A}{C_B}\right)\left(\frac{\lambda_A}{\lambda_B}\right)\frac{x_A}{x_B} \tag{2.14}$$

Similar equation written for the standard has the form

$$\frac{I_A^0}{I_B^0} = \left(\frac{C_A}{C_B}\right)\left(\frac{\lambda_A^0}{\lambda_B^0}\right)\frac{x_A^0}{x_B^0} \tag{2.15}$$

where x_A^0 and x_B^0 are the known surface concentrations of the components of the standard surface. From (2.14) and (2.15) we can derive the following system of equations

$$\frac{x_A}{x_B} = \frac{x_A^0}{x_B^0}\,\frac{(\lambda_B/\lambda_B^0)}{(\lambda_A/\lambda_A^0)}\,\frac{I_A}{I_B}\,\frac{I_B^0}{I_A^0} \tag{2.16}$$

$$x_B = 1 - x_A$$

which can be used for calculations of the surface composition. If we expect that the surface composition of the sample is reasonably close to the composition of the standard surface, we may assume that $\lambda_A \cong \lambda_A^0$ and $\lambda_B \cong \lambda_B^0$, since the inelastic mean free path is considered to be a relatively weak function of the composition. Equations (2.16) simplify to

$$\frac{x_A}{x_B} = \frac{x_A^0}{x_B^0}\,\frac{I_A}{I_B}\,\frac{I_B^0}{I_A^0} \tag{2.17}$$

$$x_B = 1 - x_A$$

As follows from (2.17), to determine the surface composition we need to measure the ratio of peak intensities for the sample and the ratio of the same peak intensities for a standard.

2.2. Quantitative analysis without standards

Best results of a quantitative analysis with standards are expected if the surface structure of the standard and the sample studied is similar. The mathematical formalism is based on the assumption that the surface is ideally flat and the analysed surfaces should be possibly close to this model. Such situation is rather exceptionally encountered in experimental practice of routine analysis. Frequently the sample surface is rough or may be in the form of a powder, which practically excludes the use of standards. Furthermore, the surface may be, in general, covered with contamination, which cannot be removed by the usual methods (sputtering, heat treatment, oxygen adsorption, *etc.*) without uncontrolled changes of the surface composition. Presence of contamination should be then accounted for in the procedure of quantitative analysis. Examples of such samples are polymers or the high T_c superconductors. The only method of quantitative analysis, which can be used in such cases, is the relative sensitivity factor approach. The corresponding formalism is very simple. We as-

sume that the signal intensity, I_i, due to any elemental constituent of the sample, is proportional to concentration

$$I_i = \phi_i x_i \tag{2.18}$$

where the proportionality coefficient, ϕ_i, is called the sensitivity factor. Thus, the concentration of i-th element is calculated from

$$x_i = \frac{I_i/\phi_i}{\sum_k I_k/\phi_k} \tag{2.19}$$

There are tabulations of the sensitivity factors available in the literature [2,8]. Furthermore, the manufacturers of the XPS instruments usually recommend a set of sensitivity factors for a given type of the spectrometer.

One can raise a number of objections concerning the accuracy of quantitative analysis based on the sensitivity factors. Firstly, the matrix effects are neglected in the above procedure. The relative sensitivity factors are usually measured for elemental solids or selected compounds, which have different electron transport properties than the studied sample. The difference should be accounted for by the corresponding values of the inelastic mean free path. Secondly, the instrumental effects are neglected. The relative sensitivity factors published in the literature or recommended by the manufacturers correspond to a certain type of instruments, while their use in processing the data collected by a different spectrometer or after changing the spectrometer settings may lead to considerable errors.

In 1991 the reliability of different procedures of quantitative XPS analysis was estimated by performing the Round Robin analysis of the same set of samples in different laboratories [9]. The Round Robin was supported by the Japanese scientists participating in the VAMAS-SCA program (Versailles Project on Advanced Materials and Standards, Surface Chemical Analysis working party). Three samples of the AuCu alloy with the bulk composition of 25, 50, and 75 at. % of Au were submitted to XPS quantitative analysis. The analysis was made by 26 participants in 19 laboratories. Prior to analysis, the sample surface was submitted to the same treatment to render the results comparable. The surface was sputtered by 2 keV Ar ions until disappearance of contamination signals. The spectra emitted by the Al Kα radiation were recorded in vicinity of Cu $2p_{3/2}$ and Au 4f peaks. Three described above procedures of quantitative analysis were applied: 1. Procedure involving two elemental standards [Eqs. (2.12) and (2.13)]; 2. Procedure involving an alloy as the standard material [Eq. (2.17)]; 3. Relative sensitivity factor approach [Eq. (2.19)].

It has been found that the procedure involving the alloy standard was the most reliable. The surface concentration x was determined with uncertainity Δx varying from

±1.41% to ±1.81% depending on the alloy. The uncertainity of surface composition for the procedure involving two elemental standards varied from ±1.74% to ±2.43%. However, the uncertainity was considerably larger for the relative sensitivity factor approach varying from ±8.82% to ±10.4%. In view of these results the question arises if it is possible at all to perform the analysis of complex materials with a good accuracy. This issue will be discussed in the following sections, devoted to different possibilities of improving the reliability of the relative sensitivity factor approach.

3. QUANTITATIVE XPS ANALYSIS OF COMPLEX SAMPLES

Different procedures for quantitative analysis of complex multicomponent solids are in fact modifications of the relative sensitivity factor approach. These modifications consist in different methods of introducing corrections accounting for the characteristics of the instrument, properties of the sample and the configuration of the experiment. The following sections provide detailed information on the most reliable correction procedures for procedures of quantitative analysis without standards.

3.1. The method of Ebel

Ebel [10] has pointed out that analogies exist between the formalism of X-ray fluorescence analysis (XRFA) and the quantitative XPS analysis. Thus, the relation between the photoelectron intensity and the surface concentration of emitting element can be obtained by proper modifications of the formalism of XRFA. For simplicity let us consider here the case of clean surface, *i.e.* the sample without the overlayer of contaminations.

As in the case of the relative sensitivity factor, the experimental procedure provides one intensity of the photoelectron peak for each element. Adjustment of the formalism of XRFA to describe the photoelectron current from the *i*th element leads to the following expression [9]

$$I_i = TD_e A_0 \Delta\Omega F_x (d\sigma_x/d\Omega)_i \frac{N_0}{A_i} \frac{c_i}{\sum_{j=1}^{n} \frac{c_j}{\rho_j^0 \lambda_{ij}^0}} \tag{3.1}$$

where N_0 is the Avogadro number, A_i is the atomic mass of the *i*th element, c_i is the concentration of *i*th element (expressed as the mass fraction), ρ_j^0 is the density of pure *j*th element, λ_{ij}^0 is the IMFP of photoelectrons emitted from *i*th atomic species in the pure *j*th element, and c_i is the concentration of *i*th component expressed as mass fraction. In (3.1) we neglect the attenuation by the layer of contamination and the influence of surface roughness. The product $T D_e A_0$ comprises properties of the instrument and is usually called the spectrometer function. This function usually depends on en-

ergy of photoelectrons, E. Let us denote the spectrometer function by $S(E)$. Taking into account (2.2), we may write the following system of equations

$$I_i = F_x \Delta\Omega S(E_i)(\sigma_x)_i W(\beta_i, \psi) \frac{N_0}{A_i} \frac{c_i}{\sum_{j=1}^{n} \frac{c_j}{\rho_j^0 \lambda_{ij}^0}} \tag{3.2}$$

$i = 1, 2, \ldots, n$

To solve this system we need to know the values of the photoelectric cross sections, σ_x, and the asymmetry parameter, β, for all photoelectron lines. They can be taken from the extensive tabulations available in [5–7,11]. We also need the values of λ_{ij} for kinetic energies of all photoelectrons in all pure elements present in the sample. These values can be found in [12,13] or in the form of a computer controlled database [14]. Next step is the determination of the spectrometer function. This problem will be addressed in further sections. Under obvious condition that

$$\sum_{i=1}^{n} c_i = 1 \tag{3.3}$$

the system of (3.2) can be solved with respect to all concentrations. Ebel [10] proposed the iterative procedure for this purpose. The starting values of concentrations can be obtained from

$${}^0c_i = \frac{I_i}{S(E_i)(\sigma_x)_i W(\beta_i, \psi) \frac{N_0}{A_i}}$$

$i = 1, 2, \ldots, n$

The resulting values are submitted then to the normalizing condition (3.3). The concentrations corresponding to the lth iteration are calculated from

$${}^lc_i = \frac{I_i}{S(E_i)(\sigma_x)_i W(\beta_i, \psi) \frac{N_0}{A_i} \sum_{j=1}^{n} \frac{{}^{l-1}c_j}{\rho_j^0 \lambda_{ij}^0}}$$

$i = 1, 2, \ldots, n$

After each iteration, concentrations are normalized to satisfy the condition (3.3).

One can prove that (3.1) is equivalent to the derived earlier (2.5). Remembering the following expressions

$$c_i = \frac{x_i A_i}{\sum_{j=1}^{n} x_j A_j} \qquad (3.4)$$

$$M_i^0 = \frac{N_0 \rho_i^0}{A_i} \qquad (3.5)$$

we can easily prove that

$$\frac{N_0}{A_i} \frac{c_i}{\sum_{j=1}^{n} \frac{c_j}{\rho_j^0 \lambda_{ij}^0}} = M \frac{x_i}{M \sum_{j=1}^{n} \frac{x_j}{M_j^0 \lambda_{ij}^0}} \qquad (3.6)$$

Comparison of (2.5) and (3.1) shows that they are equivalent, if the IMFP of photoelectrons originating from *i*th atomic species and moving in the sample material is expressed by

$$\lambda_i = \frac{1}{M \sum_{j=1}^{n} \frac{x_j}{M_j^0 \lambda_{ij}^0}} \qquad (3.7)$$

Equation (3.7) can also be expressed in terms of the mass fractions

$$\lambda_i = \frac{1}{\rho \sum_{j=1}^{n} \frac{c_j}{\rho_j^0 \lambda_{ij}^0}} \qquad (3.8)$$

where ρ is the density of the sample. This equation can be derived from (3.4), (3.5), (3.8) and taking into account the relation

$$\rho = \frac{1}{\sum_{j=1}^{n} \frac{c_j}{\rho_j^0}} \qquad (3.9)$$

The latter equation is valid under assumption that the mean volume of the atom in the sample is the same as in the pure element.

The procedure of quantitative analysis described above has one serious drawback. To solve the resulting system of equations (3.2), one has to estimate the values of λ_{ij} at energies of all photoelectrons in all pure elemental components. Sometimes

this may be a problem, *e.g.* in cases when the data on the IMFP for one or more pure components are not available, or when one or more pure components is or are gaseous (oxides, chlorides, *etc.*). Ebel *et al.* [15] has developed a modified procedure of quantitative analysis, in which the above problems can be circumvented.

Let us now consider a multicomponent sample covered with an overlayer of contamination. Equations (3.2) written for such a sample have the following form

$$I_i = F_x \Delta\Omega S(E_i)(\sigma_x)_i W(\beta_i, \psi) \frac{N_0}{A_i} \frac{c_i}{\sum_{j=1}^{n} \frac{c_j}{\rho_j^0 \lambda_{ij}^0}} \exp\left(-\frac{d}{\lambda_{il} \cos\alpha} \right) \tag{3.10}$$

$i = 1, 2, \ldots, n$

where λ_{il} is the IMFP of photoelectrons corresponding to ith component in the overlayer material, and d is the overlayer thickness. Calculations associated with quantitative XPS analysis are considerably simplified if we assume that the IMFP of ith photoelectrons in the sample material can be represented as a product of two factors: h depending only on the matrix and $f(E_i)$ depending only on the photoelectron kinetic energy E_i. Thus, (3.8) can be written as follows

$$\lambda_i = \frac{1}{\rho \sum_{j=1}^{n} \frac{c_j}{\rho_j^0 \lambda_j^0}} = h \cdot f(E_i) \tag{3.11}$$

Introducing (3.11) into (3.10), we get

$$I_i = F_x \Delta\Omega S(E_i)(\sigma_x)_i W(\beta_i, \psi) \frac{N_0}{A_i} h f(E_i) \rho \exp\left(-\frac{d}{h_l f(E_i) \cos\alpha} \right) c_i \tag{3.12}$$

$i = 1, 2, \ldots, n$

where h_l is the constant h for the overlayer material. The photoelectron current can also be related to the atom fraction instead of the mass fraction. From (3.4), (3.9), and additionally taking into account the equation

$$M = \frac{N_0}{\sum_{j=1}^{n} x_j \frac{A_j}{\rho_j^0}}$$

we obtain

$$\frac{N_0 \rho}{A_i} c_i = M x_i \tag{3.13}$$

Equation (3.12), on account of (3.13), can be transformed to the form

$$I_i = F_x \Delta\Omega S(E_i)(\sigma_x)_i W(\beta_i, \psi) h f(E_i) M \exp\left(-\frac{d}{h_l f(E_i) \cos\alpha} \right) x_i \tag{3.14}$$

$i = 1, 2, \ldots, n$

Let us group together all the parameters characteristic for the sample and for the instrument in one constant C. We have

$$I_i = C S(E_i)(\sigma_x)_i W(\beta_i, \psi) f(E_i) \exp\left(-\frac{d}{h_l f(E_i) \cos\alpha} \right) x_i \tag{3.15}$$

$i = 1, 2, \ldots, n$

where $C = F_x \Delta\Omega h M$. Ebel *et al.* [15] proposed a very simple universal energy dependence of the IMFP

$$f(E) = E^{0.7} \tag{3.16}$$

Furthermore, these authors listed very useful polynomial approximations expressing the atomic number dependence of parameters $(\sigma_x)_i$, β_i, and E_i. These dependences were estimated for all major atomic subshells. The above information makes possible calculations of the surface composition from (3.12) or (3.15). Prior to calculations, one should assume a certain value of the ratio d/h_l to establish the sensitivity of the calculated composition to the surface cleanliness. For a clean surface, we have $d/h_l = 0$. Note that we have now derived the explicit expression for the sensitivity factor. Comparison of (2.18) and (3.15) gives

$$\phi_i = C S(E_i)(\sigma_x)_i W(\beta_i, \psi) f(E_i) \exp\left(-\frac{d}{h_l f(E_i) \cos\alpha} \right) \tag{3.17}$$

The obvious way to calculate the surface composition is the use of (2.19) with (3.17).

3.2. The Multiline Analysis (MLA-1)

Usually, each elemental component of the sample may emit several photoelectron lines. If we select one photoelectron line for one elemental component, numerous

combinations of peaks are possible. Each combination of selected photoelectrons may provide somewhat different surface composition of the sample studied. A question arises if it is possible to develop a procedure of quantitative analysis, which uses simultaneously all the peaks visible in the spectra. Such problem has been addressed by Hanke *et al.* [16]. These authors proposed the term of multiline approach for the proposed procedure.

Let us summarize at first the main concepts of the multiline approach. Suppose that the sample is composed of n elements. Let atoms of ith element emit photoelectrons from m_i subshells. We will denote a particular subshell by the superscript k. Thus, the current of photoelectrons, corresponding to ith atomic species and the kth subshell, is described by [Cf. Eq. (3.12)]

$$I_i^k = F_x \Delta\Omega\, S(E_i^k)\sigma_i^k W(\beta_i^k,\psi)\frac{N_0}{A_i} h f(E_i^k)\,\rho \exp\left(-\frac{d}{h_l f(E_i^k)\cos\alpha}\right) c_i \tag{3.18}$$

where we denoted for brevity $(\sigma_x)_i^k = \sigma_i^k$. (3.18) can be transformed to the following linear equation

$$\eta_i^k = a_{0,i} + a_{1,i}\xi_i^k \tag{3.19}$$

where

$$\eta_i^k = \ln \frac{I_i^k}{\frac{1}{A_i} S(E_i^k) f(E_i^k)\sigma_i^k W(\beta_i^k,\psi)} \tag{3.19a}$$

$$a_{0,i} = \ln(const \cdot c_i) \tag{3.19b}$$

$$a_{1,i} = -d/(h_l \cos\alpha) \tag{3.19c}$$

$$\xi_i^k = 1/f(E_i^k) \tag{3.19d}$$

$$const = F_x \Delta\Omega\, h\, \rho \tag{3.19e}$$

Thus, the parameters η_i^k and ξ_i^k are expected to follow a straight line, which is characteristic for a given element. In general, the coefficients $a_{0,i}$ and $a_{1,i}$ can be determined from the linear regression. However, as the number of photoelectron lines for a given element is rather limited, it is more practical to assume certain overlayer thickness, and perform the statistical analysis only with respect to the coefficient $a_{0,i}$. Let us define the deviation due to the arbitrarily selected concentration c_i

$$\varepsilon_i^k = \eta_i^k - (a_{0,i} + a_{1,i}\xi_i^k)$$

and let us minimize the function

$$Q_i = \sum_{k=1}^{m_i} (\varepsilon_i^k)^2 \tag{3.20}$$

with respect to the coefficient $a_{0,i}$. From the condition

$$\partial Q_i / \partial a_{0,i} = 0 \qquad \text{we obtain} \qquad a_{0,i} = \frac{\sum_{k=1}^{m_i} \eta_i^k - a_{1,i} \sum_{k=1}^{m_i} \xi_i^k}{m_i}$$

The intensities of photoelectron lines, recorded for a given element, may differ and thus, they may be burdened with different statistical errors. We expect that the most reliable quantitative information can be derived from the most intense photoelectron lines, which have the smallest statistical error. To account for the difference in accuracy of the intensity determination, Hanke *et al.* [16] proposed to introduce the weight factors, G_i^k, to the above formalism. The deviations, ε_i^k, were modified according to

$$(\varepsilon_i^k)_{\text{mod}} = \varepsilon_i^k \, G_i^k \qquad \text{where} \qquad G_i^k = (I_i^k)^{1/2} \tag{3.21}$$

Such modification enhances the sensitivity of (3.20) to variations of concentrations c_i in the case of more intense lines. Thus, the function to be minimized is given by

$$Q_i = \sum_{i=1}^{n} (\varepsilon_i^k)^2 (G_i^k)^2$$

The minimization procedure provides now

$$a_{0,i} = \frac{\sum_{k=1}^{m_i} \eta_i^k (G_i^k)^2 - a_{1,i} \sum_{k=1}^{m_i} \xi_i^k (G_i^k)^2}{\sum_{k=1}^{m_i} (G_i^k)^2} \tag{3.22}$$

From (3.19b) we have

$$const = \sum_{j=1}^{n} \exp(a_{0,j}) \quad (3.23) \qquad \text{and eventually} \qquad c_i = \frac{\exp(a_{0,i})}{const} = \frac{\exp(a_{0,i})}{\sum_{j=1}^{n} \exp(a_{0,j})} \tag{3.24}$$

Equations (3.22)–(3.24), with the IMFP energy dependence described by (3.16), form the algorithm of the multiline analysis. To improve the accuracy of calculations, Hanke *et al.* [16] updated the published earlier [15] approximations for the atomic number dependence of parameters σ_i^k, β_i, and E_i. The algorithm described above will be denoted here, for the sake of convenience, by MLA-1.

3.3. The Multiline Analysis (MLA-2)

The multiline analysis algorithm has been later submitted to further modifications [17]. One can raise several objections against the algorithm MLA-1. Firstly, the weight factors, G_i^k, in the presented derivation should be associated with uncertainities ΔI_i^k rather than $\Delta\eta_i^k$, since the quantity η_i^k contains the logarithm of intensity (3.19a). Secondly, the linearization of (3.18) is not necessary, when we determine only one coefficient, $a_{0,i}$, from the statistical analysis performed for a given element. If we use (3.18) directly in the above formalism, instead of quantities η_i^k, then the weight factors given by (3.21) are justified. The correspondingly modified derivation is outlined below.

Let us express the concentrations with the atom fractions, x_i. To simplify further formalism let us denote

$$D = S(E)\,(d\sigma_x/d\,\Omega)\exp\left[-d/(h_l f(E)\cos\alpha)\right] \tag{3.25}$$

Equation (3.15) for a given photoelectron peak, with account of (3.25), can be written as follows

$$I_i^k = CD_i^k x_i$$

The deviation, due to a certain arbitrarily selected value of x_i, is given by

$$\varepsilon_i^k = I_i^k - CD_i^k x_i$$

The total deviation, Q_i^k, for the i-th element, modified with the weight factors defined by (3.21), has now the form

$$Q_i = \sum_{k=1}^{m_i} (G_i^k)^2 (\varepsilon_i^k)^2 = \sum_{k=1}^{m_i} I_i^k (I_i^k - D_i^k y_i)^2 \tag{3.26}$$

where y_i is the relative concentration

$$y_i = Cx_i \tag{3.27}$$

The correctly selected concentration, y_i, should minimize (3.26). From the condition

$$dQ_i/dy_i = 0 \qquad \text{we obtain} \qquad y_i = \frac{\sum_{k=1}^{m_i} (I_i^k)^2 (D_i^k)}{\sum_{k=1}^{m_i} I_i^k (D_i^k)^2} \tag{3.28}$$

The constant C is determined from

$$C = \sum_{i=1}^{n} y_i \tag{3.29}$$

and the concentration is calculated from (3.27). Let us denote the modified algorithm of the multiline approach by MLA-2.

As one can see, the final formulas given by (3.22)–(3.24) for the algorithm MLA-1 and (3.27)–(3.29) for the algorithm MLA-2 differ noticeably. Equations (3.27)–(3.29) seem to be better justified to use in quantitative analysis. Let us note that (3.27)–(3.29) become identical with (2.19), if only one photoelectron line is selected for each element.

In summary, the following modifications are made in the algorithm MLA-2 as compared to MLA-1:

1. The universal energy dependence of the IMFP is expressed by the Bethe equation

$$\lambda = a \frac{E}{\ln(\gamma E)} \tag{3.30}$$

instead of the exponential equation of the general form

$$\lambda = aE^p \tag{3.31}$$

The Bethe equation was found to describe better the published energy dependences of the IMFP than (3.31) [18].

2. The parameter γ describing the energy dependence of the IMFP was determined separately for different classes of materials: elemental solids, inorganic compounds, and organic compounds. This further decreases the error associated with introducing the universal energy dependence of the IMFP.

3. In the statistical analysis, the weight factors G_i^k are associated with uncertainities in the countrates I_i^k instead of uncertainities in the parameters η_i^k.

4. In applications of MLA-2, the use of the database containing all parameters necessary for calculations is recommended (photoionization cross sections, asymme-

try parameters, binding energies, atomic masses) rather than the use of fitted functions. In the algorithm MLA-1 all these data were approximated by the polynomials of atomic number. Thus, the errors associated with inaccuracy of the polynomial fit are avoided.

In the literature similar modifications of the relative sensitivity factor were proposed by other authors. One should mention that the procedure without standards of Tougaard and Jansson [19] is practically equivalent to the MLA-2 algorithm for the case of one photoelectron line selected for one element. The only difference consists in the energy dependence of the IMFP. These authors used (3.31) with the exponent 0.7, while the MLA-2 algorithm is based on the Bethe equation.

4. RELIABILITY OF QUANTITATIVE XPS ANALYSIS WITHOUT STANDARDS

As mentioned in Section 2, the reliability of the uncorrected relative sensitivity factor approach is rather poor. The uncertainities associated with concentrations found for the AuCu alloys were close to ±10% [9]. Modifications of the relative sensitivity factor approach, described in the previous section, markedly improve the accuracy of quantitative analysis. Ebel [10] applied the method based on (3.2) to a series of binary and ternary alloys of Cu, Ag, and Cu. Prior to analysis, the samples were scribed with steel wool to validate the assumption that the surface composition corresponds to the bulk composition. This made possible to verify the accuracy of quantitative XPS analysis against the results of chemical analysis of the bulk. It has been found that the averaged deviations were equal to ±2 wt%. Such accuracy is similar to accuracy of the XPS quantitative analysis using standards. Thus, the modifications introduced by Ebel [10] (account for the spectrometer function and the variations of the IMFP) significantly improve the accuracy of quantitative analysis.

Multiline approach provides also reliable results of quantitative analysis. Hanke *et al.* [16] applied the multiline analysis (MLA-1) to the sputtered Ag-Au-Cu ternary alloy. The surface composition deviated by 0.8% from the composition obtained using the chemical analysis. Such accuracy may be somewhat overestimated since certain selective sputtering effects are not excluded.

Extensive analysis of the reliability of te multiline approach (algorithm MLA-2) has been published by Jabłoński *et al.* [17]. This method was used in four laboratories equipped with different spectrometers to determine the surface composition of AuCu alloys. The test of performance of the multiline approach was based on the assumption that the surface composition of the sputtered AuCu alloy is close to the bulk composition. There is a number of indications supporting this assumption. Only slight differences from the bulk composition were obtained from statistical analysis of extensive XPS experimental material collected by the Japanese VAMAS-SCA working group [9]. Similar conclusion resulted from the analysis of the AES data recorded for the AuCu alloys sputtered with 1 keV Ar^+ ions [20]. These results are also supported by a simple criterion based on sputtering yields. The Ar sputtering

yields for Au and Cu are practically identical in wide energy range. Wehner [21] reported the same values of 2.4 at 500 eV and 3.6 at 1000 eV. The problem of selective sputtering of AuCu alloys was addressed by Tougaard and Jansson [19]. These authors have found a distinct Au enrichment at low sputter energies, 300 eV and 600 eV. However, the surface composition was, indeed, approaching the bulk composition at higher energies. Tougaard and Jansson [19] have found this result consistent with observations of other authors. Generally, it seems that the assumption of similar surface and bulk composition for AuCu alloys is justified at Ar^+ energies exceeding 1000 eV. This conclusion is also supported by the AES studies of Zhe and Tian-Sheng [22].

The method MLA-2 has been proved to be more accurate than the unmodified relative sensitivity factor approach [17]. It has been found that the average deviation between the bulk concentrations and the surface concentrations resulting from the MLA-2 algorithm was equal to 3.2 at%. This uncertainity is smaller by a factor of three from the uncertainity of the unmodified relative sensitivity factor approach reported by Yoshitake *et al.* [9]. Jabłoński *et al.* [17] also indicated that the algorithms MLA-1 and MLA-2 lead to only slightly different results of quantitative analysis. This is illustrated in Fig. 4. The difference is not large but noticeable. On close inspection, one can see that the values calculated from the MLA-2 algorithm are closer to the bulk composition than the values obtained from the MLA-1 algorithm.

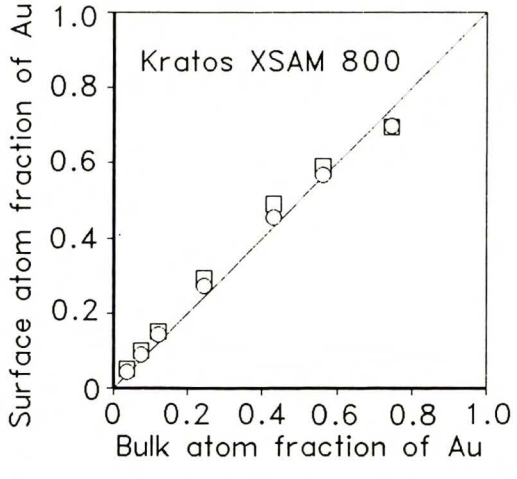

Figure 4. Surface composition of the AuCu alloys after 2 keV Ar^+ sputtering calculated from intensities measured with the Kratos XSAM 800 spectrometer. Squares: algorithm MLA-1; circles: algorithm MLA-2 (taken from Ref. 17).

The multiline approach has been used in numerous analytical applications. Quantitative analysis of the high T_c superconductor surfaces ($Bi_2Sr_2CuO_6$, $Bi_2Sr_2CaCu_2O_8$, and $YBa_2Cu_3O_7$) was based on algorithm equivalent to MLA-2 for the case of one photoelectron line selected for one element [23]. It has been found that the surface composition of the superconductor surfaces studied is in a good agreement with the

bulk composition. Quantitative XPS analysis of polyaniline doped with platinum or palladium performed with the MLA-2 algorithm indicated the enrichment of the surface region with both metals [24]. Both samples were reasonably good catalysts in the reaction of selective hydrogenation of 2-hexyne to 2-hexene, despite a relatively small content of metals in the bulk. The MLA-2 algorithm was used to control successfully the surface composition of CoPd alloys [25,26], and the compounds GaAs [27,28] and InP [28].

5. THE SPECTROMETER FUNCTION

As shown in Sections 2 and 3, the modifications of the relative sensitivity factor require the knowledge of the spectrometer function, $S(E)$. In general, the spectrometer function may depend on the spectrum acquisition mode. Consequently, it is recommended to determine this function for a given spectrometer and the mode of the analyser work rather than use the general expressions suggested for a particular type of the analyser. For this reason, we need a simple and fast method that can be frequently used in experimental practice. Different methods for determining the spectrometer function have been reviewed by Weng *et al.* [29]. Ebel *et al.* [30] have proposed a relatively simple experimental method (the so-called bias method), which is relatively convenient to use. Main features of this method are briefly outlined below.

The bias method consists in recording the spectrum intensity, I, in a narrow energy window located at energy E. The spectrum is repeatedly monitored after applying a variable potential E_{bias} to the sample. The kinetic energy of photoelectrons entering the analyser is then given by

$$E_k = E + E_{bias} \tag{5.1}$$

Let us denote by $n(E)$ the actual energy distribution of electrons emitted from the surface. We have then

$$I(E_k, E_{bias}) = S(E_k, E_{bias})n(E) \tag{5.2}$$

or, taking into account (5.1)

$$I(E + E_{bias}, E_{bias}) = S(E + E_{bias}, E_{bias})n(E) \tag{5.3}$$

After differentiating (5.3) with respect to E_{bias}, we obtain

$$\frac{dI}{dE_{bias}} = \left(\frac{\partial S}{\partial E_k} + \frac{\partial S}{\partial E_{bias}} \right) n(E) \tag{5.4}$$

where we additionally assumed that $dE_k/dE_{bias} = 1$. From (5.2) and (5.4) we eventually obtain the relation

$$\frac{d\ln I}{dE_{bias}} = \frac{d\ln S}{dE_k} + \frac{d\ln S}{dE_{bias}} \tag{5.5}$$

The derivative $d \ln I/dE_{bias}$ is determined experimentally for possibly small values of E_{bias}. This measurement is repeated for different values of E_k. Furthermore, we assume that the derivative $d \ln S/dE_{bias}$ is small and can be neglected. Solution of the resulting differential equation provides the spectrometer function.

The experimental procedures associated with determining the spectrometer function may need much effort to reach a good accuracy. In experimental practice much faster is the approximate estimation of the spectrometer function from the spectra recorded on a given spectrometer and on a spectrometer with known spectrometer function. There are software packets containing a database of the spectra, which may be used for that purpose. For example, the data processing system COMPRO (Common Data Processing System) has an option of determining the spectrometer function [31–34].

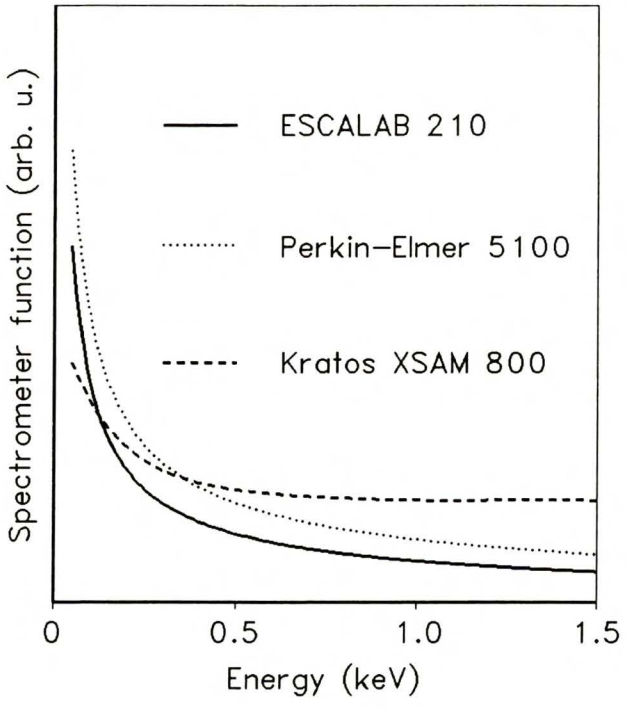

Figure 5. The spectrometer function, $S(E)$, determined for ESCALAB 210, Perkin-Elmer 5100, and Kratos XSAM 800 spectrometers (taken from [17]).

Fig. 5 shows examples of the spectrometer functions determined for several spectrometers equipped with the hemispherical analysers. As one can see, the spectrometer function varies considerably in the range of low kinetic energies, *i.e.* below 500 eV. Functions of this shape are well approximated with the expression

$$S(E) = const \times E^{-a} \tag{5.6}$$

where a is a fitted constant. For example, the function $S(E)$ determined by Zommer [35] using the bias method for the spectrometer ESCALAB 210 can be approximated by (5.6) with exponent $a = 0.72$. For the same spectrometer, the use of standard spectra from the Common Data Processing System leads to the values of $a = 0.74$ or $a = 0.69$ [35]. For some modes of work of an analyser, the general shape of the spectrometer function may be different from the shape shown in Fig. 5 [30].

6. UNIVERSAL ENERGY DEPENDENCE OF THE INELASTIC MEAN FREE PATH

As discussed in Section 3, we need a possibly universal and reliable function describing the energy dependence of the IMFP, $f(E)$, to determine the relative sensitivity factors. Knowledge of the absolute values of the IMFP is not necessary for quantitative analysis based on modified sensitivity factor approach. Due to simplicity, equation (3.31) is frequently used to describe the energy dependence of the IMFP. Despite the fact that this equation does not have the physical justification, it describes the energy dependence of the IMFP reasonably well in a relatively narrow energy range. Initially, the exponent $p = 0.5$ has been proposed for this equation [36–38]. In 1980, Wagner *et al.* [39] analysed the published experimental material and has shown that this exponent usually is larger than 0.5. They postulated the range from 0.53 to 0.80 for the exponent p. Similar conclusion resulted from other studies. Ashley and Tung [40] fitted (3.31) to the IMFP values for selected elements and compounds and have found that the exponent p ranges from 0.53 to 0.85. Reich *et al.* [41] calculated the IMFPs for carbon, silicon, germanium, Al_2O_3, SiO_2 and GeO_2, and they fitted the calculated IMFPs with (3.31). They found that the range of variation of the exponent p is slightly smaller, *i.e.* from 0.736 to 0.892. Ebel *et al.* [42] listed values of p for organic materials and indicated that they vary considerably. The largest value of p was 1.98.

Since the exponent p seems to be material and energy dependent, one has to average different values of p for a number of materials and energies. Several averaged values were proposed in the literature. The average value of $p = 0.7$ was proposed by Ebel *et al.* [15] to use in modified relative sensitivity factor method. Hanke *et al.* [16] proposed the value of 0.723 for use in calculations of the method MLA-1. Average values of 0.73 or 0.800 were found by Ebel *et al.* [43].

There are two main problems with the use of (3.31) in calculations of quantitative XPS. The range of published values of the exponent p is rather large and the averaged

value obviously depends on the averaging procedure used. A single universal value of p may not be applicable to some classes of materials. Second problem is associated with the sources of the data on the IMFP used in averaging. Majority of the experimental IMFP values originated from measurements of the AES or XPS signal attenuation due to deposition of overlayers of known thickness. The theoretical IMFPs were obtained from calculated distribution of electron energy losses in the solid. While the theoretical sources provide the IMFP values in agreement with the definition, the values resulting from the overlayer experiments are now known to be different from the IMFP. They are called the attenuation lengths (AL) and may differ from the IMFP by up to 30% or even more for some geometries [44–46]. Generally, these terms are discussed in recent reviews [13,46]. In effect, the exponents p derived from the data measured in overlayer experiments may be not suitable to describe the energy dependence of the IMFP. It has been shown that the only experimental method providing the "true" IMFP values is based on measurements of the elastic backscattering probability from surfaces [13]. This method is usually associated with the acronim EPES (Elastic Peak Electron Spectroscopy). Recently, Powell and Jabłoński [13] compiled a list of exponents p derived from EPES for 24 elements. It has been found that the exponent varies in wide range from 0.383 to 0.919. Thus, it seems that the concept of a single universal p value applicable to all solids may not be valid.

Jabłoński [18] proposed to determine the energy dependence of the IMFP separately for different classes of materials, *i.e.* elements, inorganic compounds and the organic compounds. In addition to (3.31), the Bethe equation has been considered to describe the energy dependence of the IMFP.

$$\lambda = \frac{E}{E_p^2 \beta_0 \ln(\gamma E)} \tag{6.1}$$

where E_p^2 is the free-electron plasmon energy and β_0 and γ are the material dependent parameters. This equation is obviously equivalent to (3.30). Similarly as in the case of (3.31), we need only one parameter γ to describe the energy dependence of the IMFP. An extensive database of the IMFP values published by Tanuma *et al.* for elements [12], inorganic compounds [47] and organic compounds [48] has been used as a reference for determining the parameter p in (3.31) and the parameter γ in (3.30). Both parameters were adjusted so that the deviation from the IMFP values of Tanuma *et al.* within a particular class of materials was the smallest. The fitted parameters p and γ are listed in Table 1. As one can see, the values of the parameter p obtained in the present work for elements and inorganic compounds well agree with the universal value of 0.723 recommended for use with the MLA-1 algorithm. Both fitted parameters depend noticeably on the class of materials and it is advisable to use a value suitable to an analysed sample rather than a single universal value. Jabłoński [18] has also shown that the Bethe equation better describes the energy dependence of the IMFP than

(3.31). The above recommendations are accounted for in the algorithm of multiline analysis MLA-2. Other recommendation is to select for quantitative XPS analysis the photoelectron lines with kinetic energy exceeding 500 eV. For such energies, (3.30) describes the energy dependence of the IMFPs with accuracy of 2–3%. Larger deviations are observed at lower energies.

Table 1. Values of the parameters p and γ fitted to the IMFPs of Tanuma *et al.* [12,47,48] for different classes of materials.

Class of materials	p	γ 1/eV
Elements	0.7283	0.05359
Inorganic compounds	0.7234	0.05046
Organic compounds	0.7665	0.09554
All materials	0.7414	0.06403

One should also mention that the parameters p and γ listed in Table 1 are derived from the database of IMFPs applicable to the bulk of the solid, since such IMFPs are obtained from the theoretical method based on the optical data [12,47,48]. In the surface region submitted to the XPS analysis, the mechanism of energy loss may be different than in the bulk , *e.g.* due to additional excitations of the surface plasmons. For this reason, the values of the IMFPs for the surface region may be somewhat different than in the bulk. This problem has been recently discussed by Powell and Jabłoński [13]. The only experimental method, providing the IMFPs for the surface region (in contrast to attenuation lengths) is the EPES method. However, the published IMFP values obtained from the EPES method exhibit a considerable scatter, which may be associated with deficiencies of the theoretical model used in calculations [13,49]. Furthermore, there is a limited set of IMFPs published for organic and inorganic materials. When the performance of the EPES method is improved, the resulting IMFPs would be a good basis for determination of the energy dependence for the surface region.

7. PHOTOELECTRON ELASTIC COLLISIONS

We indicated in Section 2 that the mathematical formalism of XPS is derived on the assumption that the photoelectron trajectory in a solid is linear (Cf. assumption no 4). In effect, angular distribution of emission from atomic species in the surface region (photoelectric cross section) determines the angular distribution of photoemission from the solid surface. In reality, photoelectrons may be elastically scattered on atoms of a solid. This process may modify the photoelectron trajectories and consequently affect the angular distribution of photoemission. For this reason we may expect, that the neglect of elastic photoelectron collisions may influence results of quantitative XPS analysis. This problem was originally approached over 20 years ago by Baschenko and Nefedov [50]. Until present time, numerous studies of the elastic

scattering effects were published in the literature. The published material has been reviewed by Jablonski [51] and Tilinin *et al.* [52].

In majority of published reports, the influence of elastic scattering on photoelectron angular distribution has been studied by Monte Carlo simulations of photoelectron trajectories in the solid. It has been found that the elastic photoelectron collisions can be accounted for in the formalism of XPS with two correction parameters: Q_x and β_{eff} [53,54]. These parameters modify the photoelectric cross section given by (2.2) to the form

$$(d\sigma_x/d\Omega)_{mod} = \sigma_x Q_x W(\beta_{eff}, \psi) = \sigma_x Q_x \frac{1}{4\pi}\left[1 - \frac{\beta_{eff}}{4}(3\cos^2\psi - 1)\right] \tag{7.1}$$

To account for elastic scattering effects in quantitative XPS analysis, one can use the formalism presented in Sections 2 and 3, in which the photoelectric cross section $d\sigma_x/d\Omega = \sigma_x W(\beta,\psi)$ is replaced with the modified cross section given by (7.1). The correction factors Q_x and β_{eff} for numerous elements, photoelectron lines and the experimental geometries were determined from the Monte Carlo simulations of photoelectron transport [54]. The calculated values can be approximated by the expression of the form

$$\beta_{eff} = a_1\cos^2\alpha + a_2\cos\alpha + a_3 \tag{7.2a}$$

$$Q_x = b_1\cos^2\alpha + b_2\cos\alpha + b_3 \tag{7.2b}$$

Extensive tabulation of the fitted constants a_i and b_i is available in [54].

Jabłoński and Tilinin [55] described the elastic scattering effects in XPS analytically from the approximate solution of the Boltzmann equation, using the so-called transport approximation. It has been confirmed that two parameters, Q_x and β_{eff}, are sufficient to account for elastic scattering effects. Simple expressions for these parameters were derived [55,56]

$$Q_x = (1-\omega)^{1/2} H(\cos\alpha,\omega) \tag{7.3a}$$

$$\beta_{eff} = \frac{(1-\omega)\beta}{Q_x} \tag{7.3b}$$

$$\omega = \frac{1}{1+\zeta} \tag{7.3c}$$

where $H(\mu,\omega)$ is the H function of Chandrasekhar [57], and ζ is the ratio of the electron transport mean free path to the inelastic mean free path, $\zeta = \lambda_{tr}/\lambda$. The definition of the transport mean free path, λ_{tr}, and the methods of evaluation are discussed by Jabłoński [58]. The ratios ζ for electron energy E can be estimated from the expression [56]

$$\zeta = \exp\left[\sum_{k=0}^{3}\sum_{n=0}^{3} a_{kn} Z^n (\ln E)^k\right] \tag{7.4}$$

where Z is the averaged atomic number of the solid and $a_{k\,n}$ are the universal constants. They are listed in Table 2. The correction parameters Q_x and β_{eff} calculated from (7.3) and (7.4) compare very well with values resulting from the Monte Carlo simulations. This has been observed for several photoelectron lines [55,56]. An example of such comparison is shown in Fig. 6.

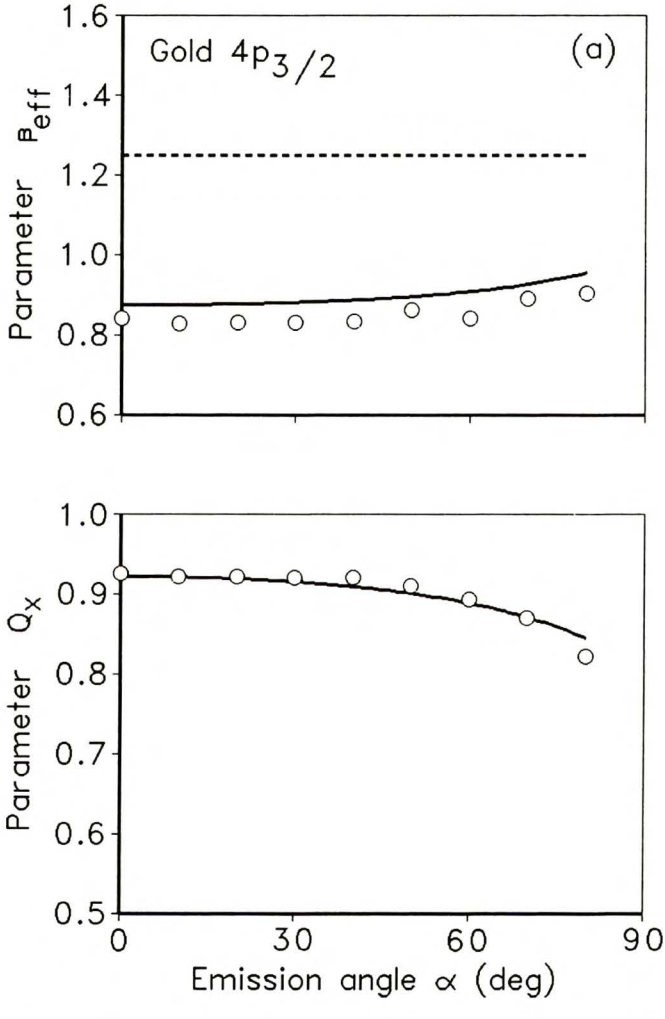

Figure 6. Dependence of the correction parameters β_{eff} and Q_x on the emission angle, α. Solid line: equations (7.3); dashed line: the asymmetry parameter, β [6] circles: Monte Carlo calculations [53]. (a) Au $4p_{3/2}$ photoelectron line; (b) Au $4f_{7/2}$ photoelectron line.

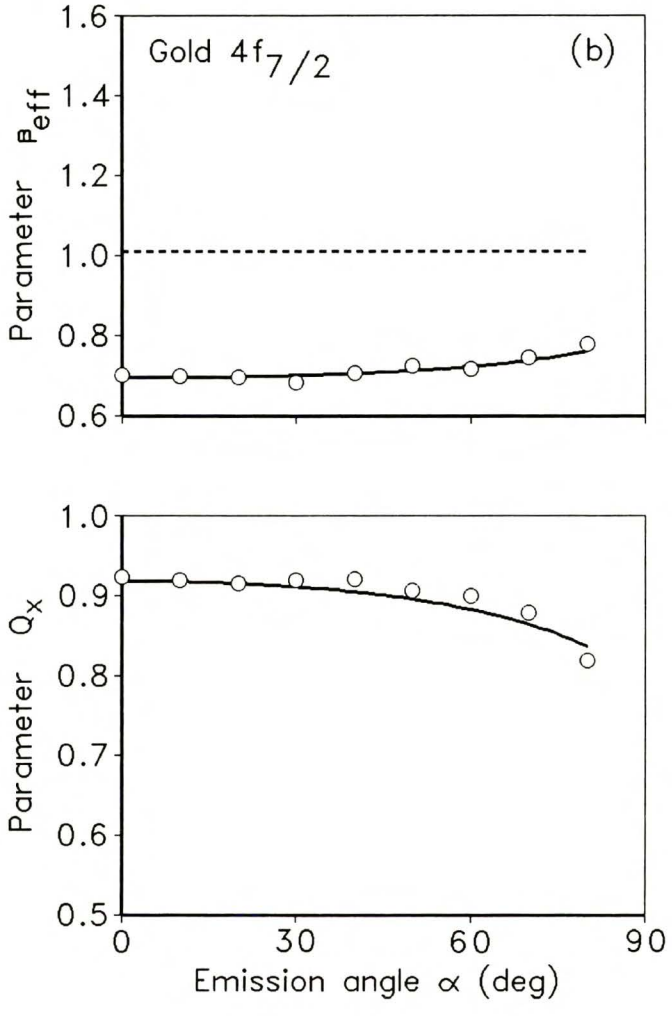

Figure 6. (continuation)

Table 2. Values of the universal constants a_{kn} for calculating the ratios $\zeta = \lambda_n/\lambda$ from (7.4).

	n = 3	n = 2	n = 1	n = 0
k = 3	-3.21438×10^{-6}	4.15715×10^{-4}	-1.10184×10^{-2}	6.47105×10^{-2}
k = 2	5.74021×10^{-5}	-7.50284×10^{-3}	0.201522	−1.13552
k = 1	-3.34967×10^{-4}	4.44227×10^{-2}	−1.22881	7.40525
k = 0	6.30016×10^{-4}	-8.46984×10^{-2}	2.40871	−15.4421

We see that the correction factors are weakly dependent on the detection angle, α, except for the range of large detection angles. The effective asymmetry parameter, β_{eff}, is generally smaller than the asymmetry parameter, β, describing the angular

distribution of photoemission from atoms. This is obviously due to the partial randomization of photoelectron trajectories by elastic photoelectron collisions. For the fully randomized directions, the asymmetry parameter is equal to zero. Slightly larger difference between the correction parameters resulting from the Monte Carlo simulations and calculated from (7.3) is found for the photoelectron lines of highest asymmetry, *i.e.* originating from the *s*-shells. Parameter β_{eff} calculated from (7.3b) is then overestimated by about 10%. Generally, (7.1) with (7.2) or (7.3) are recommended for calculations of quantitative XPS, since the angular distribution of photoemission determined with account of elastic scattering better compares with the experimental angular distribution than prediction of the uncorrected formalism [59].

8. SOFTWARE PACKET MULTI

Calculations associated with the multiline method, especially in the case when elastic scattering is accounted for, are considerably more involved as in the case of the unmodified relative sensitivity factor approach. However, application of the multiline method, as well as any other modification of the relative sensitivity factor approach, improves the reliability of the quantitative analysis. On the other hand, more complex formalism and the additional input parameters necessary for calculations make the modified approach difficult to use for routine analyses.

A useful tool to facilitate applications of the modified relative sensitivity factor approach would be a user friendly software performing all operations associated with the quantitative analysis and applicable to a possibly wide range of samples. In fact, an effort has been made in the Institute of Physical Chemistry of the Polish Academy of Sciences to develop a software packet MULTI implementing the formalism of the multiline approach MLA-2. Main features of this software are the following:

1. Implementation of the database of parameters necessary for calculations (photoelectron kinetic energies, asymmetry parameters, and photoelectric cross sections).

2. Applicability to typical classes of materials: alloys, inorganic compounds, and organic compounds.

3. Spectra processing feature, *i.e.* integration of spectra after suitable background subtraction. As an alternative, the intensities from external integration programs can be used in calculations.

4. Graphical presentation of the calculated surface composition (pie-slice plots) with concentrations expressed as the mass fractions or the atom fractions.

5. Creation of files with plots, with a possibility of printing the graphics.

6. Creation of files with complete information on quantitative analysis (all input parameters, all data taken from the database and the resulting concentrations).

7. Applicability to two typically used radiations (Mg Kα and Al Kα).

8. A possibility of including or neglecting the elastic photoelectron collisions in calculations of surface composition (implementation of (7.3)). In this way, one can evaluate the elastic scattering effects for the sample considered.

The title screen and the main menu of the MULTI software are shown in Fig. 7. An example of the graphical presentation of results is demonstrated in Fig. 8. This plot shows the calculated surface composition of polyaniline doped with palladium [24].

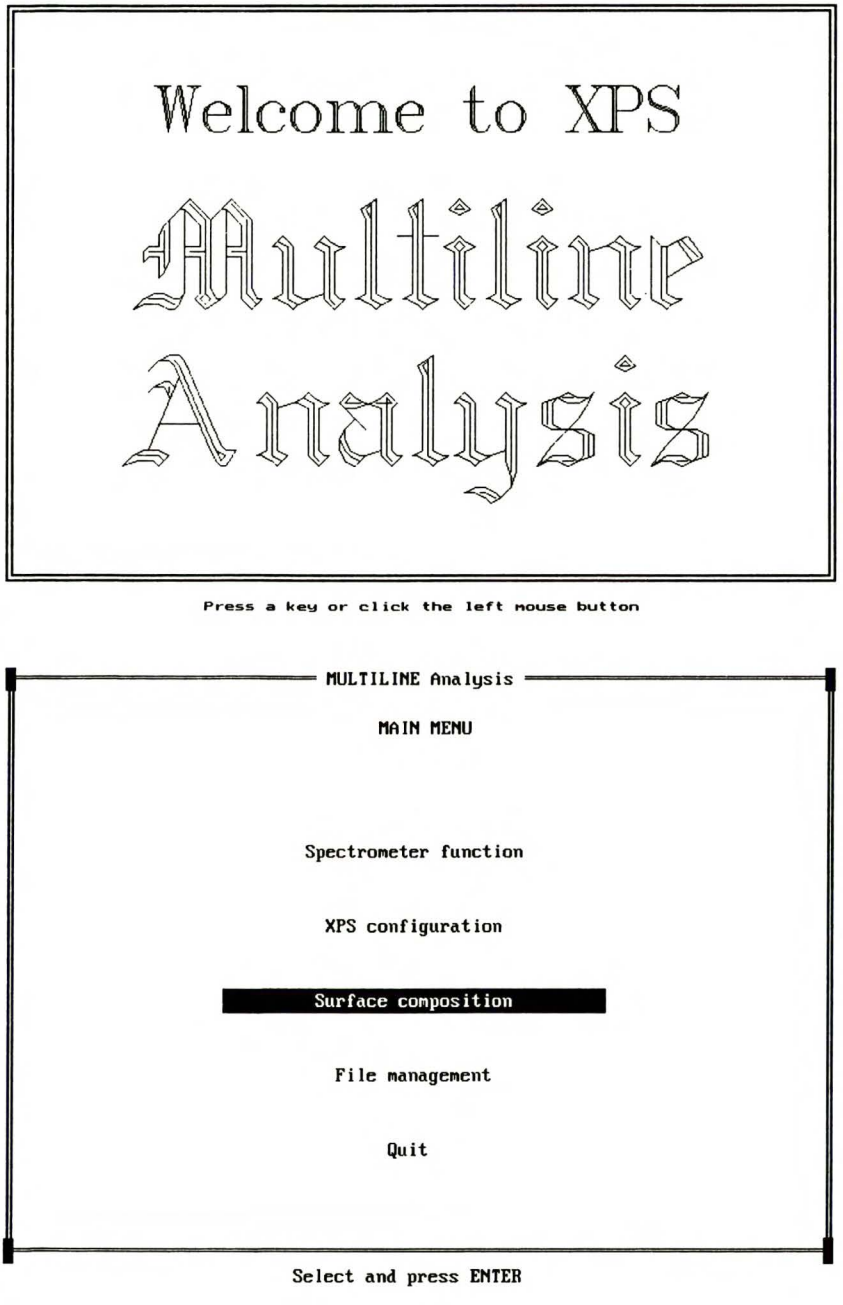

Figure 7. Opening screens of the software packet MULTI. (a) The title screen; (b) the main menu.

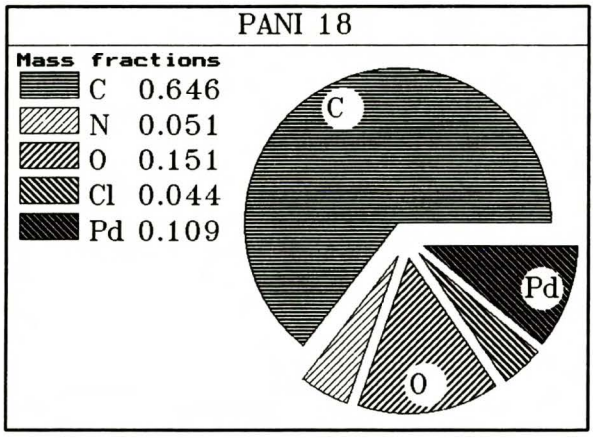

Figure 8. Graphical representation of surface composition of polyaniline doped with palladium calculated with the program MULTI (details are published in [24]).

One should stress a full portability of the MULTI software to any XPS spectrometer. The customization to a particular spectrometer consists in introducing, by one of the options, the details of the spectrometer function and the experimental configuration used for measurements. For interested laboratories this program is distributed free of charge [60].

9. CONCLUDING REMARKS

The above overview of procedures for quantitative XPS analysis indicates that there is a number of problems still to be solved. Mathematical formalism used in XPS analysis oversimplifies the photoelectron transport in solids. There is a need to account for the multiple scattering events along electron trajectories in a solid. Generally, the assumptions, on which the formalism is based (Cf. Section 2), may not always be true. We know now that the attenuation of photoelectron in the matter may be nonexponential in some cases [44,46,52]. Furthermore, the assumption of uniform composition within the sampling depth of XPS may be not valid for some samples. There are indications that the segregated layer at surfaces of binary alloys may have a complex structure. For example, composition of the first atomic layer at the surface of the equilibrated AuCu alloy differs considerably from the composition of the second layer [61]. In such a case, the presented methods of quantitative analysis would provide the composition averaged over the sampling depth of photoelectrons selected for analysis. There are other analytical procedures of XPS for determining the actual in-depth concentration profiles, which were not discussed in the present work. One possibility is to perform the XPS analysis, while removing the consecutive atomic layers during by sputtering with Ar^+ ions. However, one should be aware of the fact that the beam of ions may affect the composition within the thickness of several layers. The information on the in-depth concentration profile can also be derived from nondestructive measurements of the photoelectron intensities at different emission angles. The latter technique is denoted with the acronim ARXPS (Angle-Resolved

X-ray Photoelectron Spectroscopy). Extensive review of this technique has been published by Cumpson [62]. The interested reader is referred to this work. Finally, it should be mentioned that the in-depth profile can be roughly estimated from the shape of the background in the vicinity of the photoelectron peak [63–65]. However, the formalism of the spectra processing is then very complex. Practical applications of this approach are facilitated with a specialized software packet QUASES [66].

Acknowledgment*

This work has been partially supported by the Polish State Committee for Scientific Research (Grant no 2P03B 039 18).

REFERENCES

1. Siegbahn K., Nordling C., Fahlman A., Nordberg R., Hamrin K., Hedman J., Johansson G., Bergmark T., Karlsson S.-E., Lindgren I., and Lindberg B., ESCA. Atomic, Molecular and Solid State Structure Studied by Means of Electron Spectroscopy", Almqvist and Wiksells, Uppsala, 1967.
2. Practical Surface Analysis. Vol. 1., *Auger and X-ray Photoelectron Spectroscopy*, Edited by Briggs D. and Seah M.P., J. Wiley, Salle+Sauerländer, Chichester, 1990.
3. Fadley C.S., Baird R.J., Siekhaus W., Novakov T. and Bergström S.A.L., *J. Electron Spectrosc. Relat. Phenom.*, **4**, 93 (1974).
4. Cooper J.W. and Manson S.T., *Phys. Rev.*, **177**, 157 (1969).
5. Reilman R.F., Msezane A. and Manson S.T., *J. Electron Spectrosc. Relat. Phenom.*, **8**, 389(1976).
6. Band I.M., Kharitonow Yu.I. and Trzhaskovskaya M.B., *Atomic Data Nucl. Data Tables*, **23**, 443 (1979).
7. Yeh J.J. and Lindau I., *Atomic Data Nucl. Data Tables*, **32**, 1 (1985).
8. Wagner C.D., Davis L.E., Zeller M.V., Taylor J.A., Raymond R.H. and Gale L.H., *Surface Interface Anal.*, **3**, 211(1981).
9. Yoshitake M., Yoshihara K. and other members of the VAMAS-SCA working group in Japan, *Surface Interface Anal.*, **17**, 711 (1991).
10. Ebel M.F, *Surface Interface Anal.*, **1**, 58 (1979).
11. Scofield J.H., *J. Electron Spectrosc. Relat. Phenom.*, **8**, 129 (1976).
12. Tanuma S., Powell C.J. and Penn D.R., *Surface Interface Anal.*, **17**, 911 (1991).
13. Powell C.J. and Jabłoński A., *J. Phys. Chem. Ref. Data*, **28**, 19 (1999).
14. Powell C.J. and Jabłoński A., NIST Electron Inelastic-Mean-Free-Path Database (SRD 71), U.S. Department of Commerce, National Institute of Standards and Technology, Gaithersburg, Maryland (1999).
15. Ebel M.F., Ebel H. and Hirokawa K., *Spectrochim. Acta*, **B37**, 461 (1982).
16. HankeW., Ebel H., Ebel M.F., Jabłoński A. and Hirokawa K., *J., Electron Spectrosc. Relat. Phenom.*, **40**, 241 (1986).
17. Jabłoński A., Lesiak B., Zommer L., Ebel M.F., Ebel H., Fukuda Y., Suzuki Y. and Tougaard S., *Surface Interface Anal.*, **21**, 724 (1994).
18. Jabłoński A., *Surface Interface Anal.*, **20**, 317 (1993).
19. Tougaard S. and Jansson C., *Surface Interface Anal.*, **20**, 1013 (1993).
20. Yoshihara K., Shimizu R., Homma T., Tokutaka H., Goto K., Fujita D., Kurokawa A., Ichimura S., Kurahashi M., Kudo M., Hashiguchi Y., Suzuki T., Ohmura T., Soeda F., Tanaka K., Tanaka A., Sekine T., Shiokawa Y. and Hayashi T., *Surface Interface Anal.*, **16**, 140 (1990).
21. Wehner G.K., in: Methods of Surface Analysis, edited by Czanderna A.W., Elsevier, Amsterdam, 1975, p. 11.
22. Zhe Q. and Tian-Sheng X., *Surface Sci.*, **194**, L127 (1988).

* The author's fee was financed by the Association for Author Rights Collective Administration of Scientific and Technical Works KOPIPOL with a seat in Kielce from the remuneration collected on the basis of Art. 20 of the Law on Author Right and Related Rights.

23. Jabłoński A., Sanada N., Suzuki Y., Fukuda Y. and Nagoshi M., *J. Electron Spectrosc. Relat. Phenom.*, **63**, 131 (1993).
24. Sobczak J.W., Lesiak B., Jabłoński A., Kosiński A. and Palczewska W., *Polish J. Chem.*, **69**, 1732 (1995).
25. Lesiak B., Zemek J., de Haan P. and Jozwik A., *Surface Sci.*, **346**, 79 (1996).
26. Krawczyk M., Zommer L., Lesiak B. and Jabłoński A., *Surface Interface Anal.*, **25**, 356 (1997).
27. Krawczyk M., Jabłoński A., Tougaard S., Toth J., Varga D. and Gergely G., *Surface Sci.*, **402–404**, 451 (1998).
28. Zommer L., Lesiak B., Jabłoński A., Gergely G., Menyhard M., Sulyok A. and Gurban S., *J. Electron Spectrosc. Relat. Phenom.*, **87**, 177 (1998).
29. Weng L.T., Vereecke G., Genet M.J., Bertrand P. and Stone W.E.E., *Surface Interface Anal.*, **20**, 179 (1993).
30. Ebel H., Zuba G. and Ebel M.F., *J. Electron Spectrosc. Relat. Phenom.*, **31**, 123 (1983).
31. Yoshihara K., Yoshitake M. and the VAMAS-SCA Community, *Surface Interface Anal.*, **18**, 724 (1992).
32. Yoshihara K. and Yoshitake M., *J. Vac. Sci. Technol.*, **A12**, 2342 (1994).
33. Yoshihara K. and Yoshitake M., *J. Vac. Sci. Technol.*, **A16**, 1388 (1998).
34. More information on the Common Data Processing System is available at the web address: *http://sekimori.nrim.go.jp*.
35. Zommer L., *Vacuum*, **46**, 617 (1995).
36. Chang C.C., *Surface Sci.*, **48**, 9 (1975).
37. Pons F., Le Hericy J. and Langeron J.P., *Surface Sci.*, **69**, 565 (1977)
38. Seah M.P. and Dench W.A., *Surface Interface Anal.*, **1**, 2 (1979).
39. Wagner C.D., Levis L.E. and Riggs W.M., *Surface Interface Anal.*, **2**, 53 (1980).
40. Ashley J.C. and Tung C.J., *Surface Interface Anal.*, **4**, 52 (1982).
41. Reich T., Yarzemski V.G. and Nefedov V.I., *J. Electron Spectrosc. Relat. Phenom.*, **46**, 255 (1988).
42. Ebel M.F., Ebel H., Puchberger C. and Svagera R., *J. Electron Spectrosc.*, **57**, 357 (1991).
43. Ebel H., Ebel M.F., Baldauf P. and Jabłoński A., *Surface Interface Anal.*, **12**, 172 (1988).
44. Jabłoński A. and Tougaard S., *J. Vac. Sci. Technol.*, **A8**, 106 (1990).
45. Cumpson P.J. and Seah M.P., *Surface Interface Anal.*, **25**, 430 (1997).
46. Jabłoński A. and Powell C.J., *J. Electron Spectrosc. Relat. Phen*om., **100**, 137 (1999).
47. Tanuma S., Powell C.J. and Penn D.R., *Surface Interface Anal.*, **17**, 927 (1991).
48. Tanuma S., Powell C.J. and Penn D.R., *Surface Interface Anal.*, **20**, 77 (1993).
49. Jabłoński A. and Jiricek P., *Surface Sci.*, **412/413**, 42 (1998).
50. Baschenko O.A. and Nefedov V.I., *J. Electron Spectrosc. Relat. Phenom.*, **17**, 406 (1979).
51. Jabłonski A., *Surface Interface Anal.*, **14**, 659 (1989).
52. Tilinin I. S., Jabłoński A. and Werner W.S.M., *Progress Surface Sci.*, **52**, 193 (1996).
53. Jabłoński A. and Powell C.J., *Phys. Rev.*, **B50**, 4739 (1994).
54. Jabłoński A., *Surface Interface Anal.*, **23**, 29 (1995).
55. Jabłoński A. and Tilinin I.S., *J. Electron Spectrosc. Relat. Phenom.*, **74**, 207 (1995).
56. Jabłoński A., *Surface Sci.*, **364**, 380 (1996).
57. Chandrasekhar S., Radiative Transfer, Dover Publications, Inc., NY, 1960, Chapter 5.
58. Jabłoński A., *Phys. Rev.*, **B58**, 16470 (1998).
59. Jabłoński A. and Zemek J., *Phys. Rev.*, **B48**, 4799 (1993).
60. For more information, contact A. Jablonski, Institute of Physical Chemistry, Warsaw, Poland, e-mail: jablo@ichf.edu.pl.
61. Mróz S., *Progress Surface Sci.*, **59**, 323 (1998).
62. Cumpson P.J., *J. Electron Spectrosc. Relat. Phenom.*, **73**, 25 (1995).
63. Schleberger M., Fujita D., Scharfschwerdt C. and Tougaard S., *J. Vac. Sci. Technol.*, **B13**., 949 (1995).
64. Tougaard S., *J. Vacuum Science Technol.*, **A14**, 1415 (1996).
65. Tougaard S., *Surface Interface Analysis*, **26**, 249 (1998.)
66. More information is available at the web address: *http://www.quases.com*